Final Report:
Impacts of tidal energy extraction on sediment dynamics in Minas Basin, Bay of Fundy, NS

Research Project #: 300-170-09-13
31 December, 2012

Peter C. Smith, Gary Bugden, and Yongsheng Wu
Bedford Institute of Oceanography
Fisheries & Oceans Canada
Dartmouth, NS Canada
and
Ryan Mulligan, Queens University
Kingston ON, Canada
and
Jing Tao, Dalhousie University
Halifax, NS Canada
Submitted on: January, 2013

Summary

The introduction of in-stream turbines in Minas Channel could impose changes to the oceanographic conditions on the tidal flats, at the shoreline, and in river channels in Minas Basin that might result in sediment erosion/accretion as the system adjusts to a new equilibrium. The goal of this research project is the development of numerical hydrodynamic and sediment transport models for Minas Basin in the Bay of Fundy, the focus of which will be the sediment dynamics of the tidal inlets and flats. The models have been validated by field observations and used for prediction of the impacts of tidal power devices on the dynamics of coastal flows, sediment transport and seabed morphology. These models include the relevant physical processes for sediment dynamics, including tidal currents, river flows and wave-induced sediment mobilization and re-suspension. The models used for this study are the first step in addressing the problem of sedimentation in tidal rivers and on the tidal flats induced by tidal energy extraction.

The models are based on existing and well established in three-dimensional models for hydrodynamics (Delft3D and FVCOM), and use coupled nested grids or unstructured meshes to appropriately resolve the locations of interest within Minas Basin. Model grids have been developed using existing high-resolution multi-beam bathymetry (Parrott *et al*, 2008). Relevant forcing mechanisms are evaluated and included, for example tides, storm surges, winds and waves. The model results have been used to evaluate sediment erosion, suspension, transport and deposition. The domain encompasses all of Minas Basin, with the boundary placed in Minas Passage such that changes in boundary conditions may be used to represent various tidal energy extraction schemes. The impacts of single turbines, lines and arrays of turbines are simulated in the model flows as well. Regarding validation of the natural system, the models are used to predict sediment changes during the spring/neap tidal cycle and compared with data reported by Amos and Joice (1977) and concurrent observations by others, including measurements of sediment concentration profiles, erosion and deposition rates in sensitive estuaries of the Avon and Cornwallis Rivers and nearby tidal flats in the upper Bay of Fundy. The predicted differences between spring and neap conditions are used as a proxy for before and after tidal energy extraction. The modelling system was used to predict changes to tidal currents, water levels, sediment concentrations, sediment transport rates and areas of seabed erosion/accretion. This research identifies some of the impacts of tidal power generation on the coastal marine environment in Minas Basin, which benefits and complements other environmental research.

Scientific Objectives

The scientific objectives of this project are:

1. To obtain strategic observations of hydrodynamic circulation and salient features of the sediment regime in the Upper Bay of Fundy.
2. To develop two high-resolution hydrodynamic models (FVCOM, Delft3D) validated against current and sea level observations.
3. To develop two high-resolution sediment dynamics models (FVCOM, Delft3D) validated against observations of the sediment regime, e.g. erosion and deposition rates.
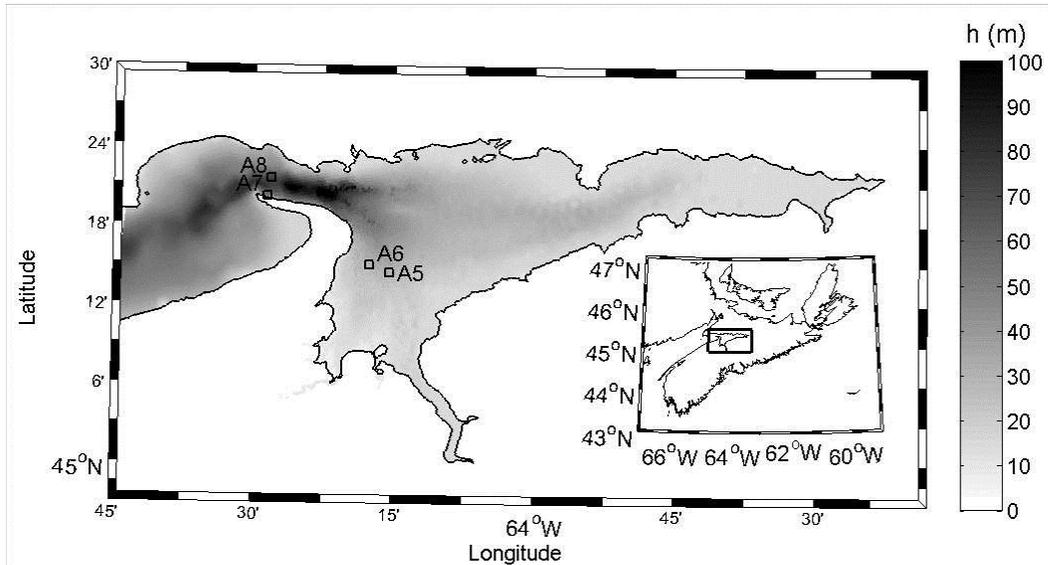
Figure 1a: Location map (inset) and bathymetry of Minas Channel and Minas Basin covering the Delft3D model domain. Selected instrument locations (deployments in July-August 2009), used for Delft3D validation, are indicated.

Description of Progress

With respect to the objectives stated above, the following results have been obtained:

1. Observations of Hydrodynamic and Sediment Regimes in the Upper Bay of Fundy:

Ocean current observations have been collected, processed and quality controlled at a total of eight sites(A1-A8) in the upper Bay of Fundy (Minas Passage, Minas Basin) to complement the industry measurements collected by FORCE in the NW corner of the Passage (see Figure1b below). Furthermore suspended sediment (Total Suspended Matter or TSM) profiles have been obtained at the A5 location.
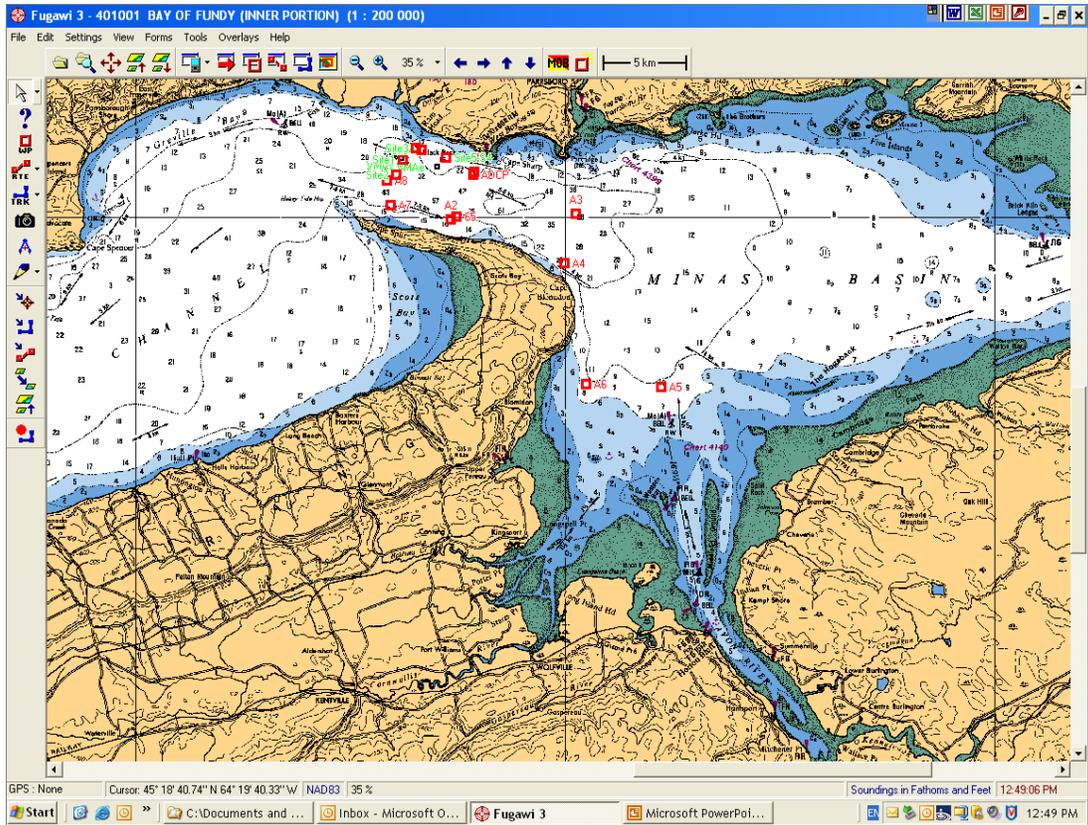
A1: 45^0 21' 23.34" N A2: 45^0 20.00' N A3: 45^0 20.00' N A4: 45^0 18.50'N FORCE 45^0 22.00' N
         64^0 24' 13.80" W 64^0 25.00' W 64^0 20.00'W 64^0 20.00'W sites near 64^0 25.50' W
A5: 45^0 14.40' N   A6: 45^0 14.58' N A7: 45^0 20.38' N A8: 45^0 21.20' N:
         64^0 15.50' W 64^0 19.00' W 64^0 28.08'W 64^0 28.25' W

Figure 1b Mooring locations for current and sediment observations in Minas Basin and Minas Passage.

Ocean colour imagery of the upper Bay continued to be collected from the MERIS satellite, quality controlled and analyzed until MERIS recently ceased to function. Using an algorithm developed for similar data from the Northumberland Strait, these satellite data have been converted to surface suspended particulate matter (Figure 2a) and validated with selected sediment concentration observations collected at various locations in the upper Bay. Furthermore, a time series of the mean value of the total suspended matter at the A5 site (see Fig.1), derived from a 3X3 pixel box of MERIS FR level2 TSM product and validated with *in situ* surface data, reveal a strong seasonal cycle in surface sediment concentration, with a maximum in winter (Jan.-Apr, Figure 2b), as well as significant inter-annual variability (winter, 2009 vs. winter, 2010).
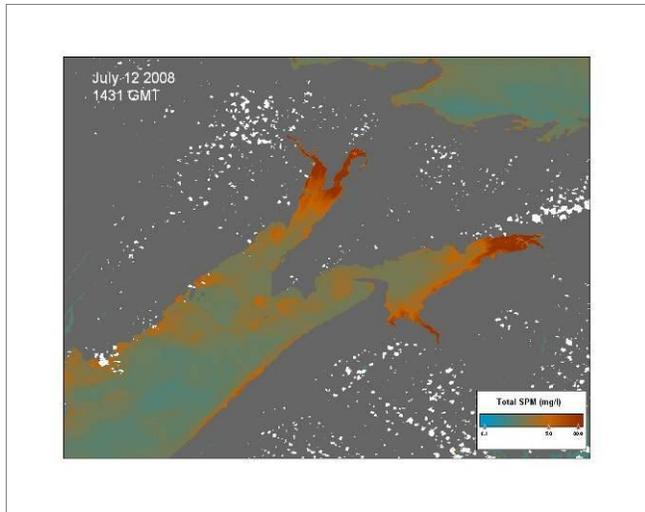
Figure 2a. Estimates of total suspended particulate matter (TSM; mg/l) derived from a MERIS image of the upper Bay of Fundy on July 12, 2008.
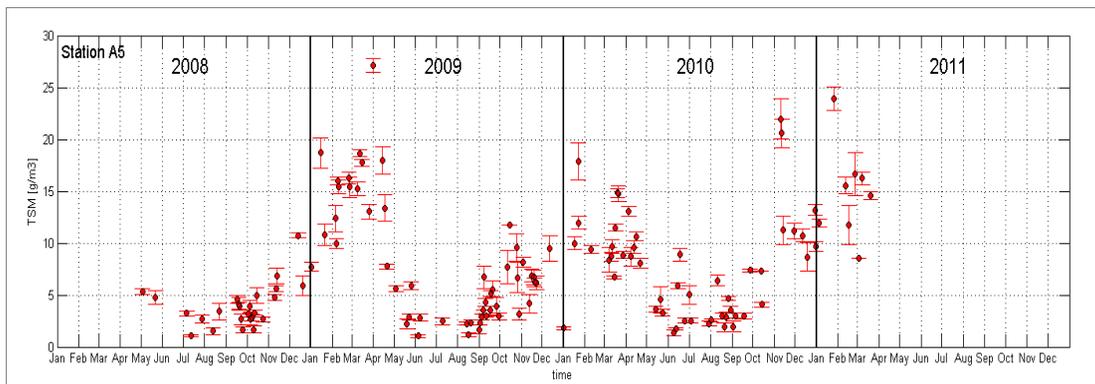
Figure 2b. Mean values of TSM over a 3X3 pixel box (~1 sq.km.) surrounding the A5 mooring site off the mouth of the Avon River.

In March 2011 a mooring package containing two ADCP's of different frequencies was deployed at site A5. An anchor station was occupied nearby for a portion of a tidal cycle and observations including: discrete water samples at several depths for TSM, CTD profiles (with an OBS), water column optics with a Hyperprobe and particle size spectra using a LISST and silhouette camera were collected to characterize winter conditions. The anchor station was repeated in June just prior to mooring recovery to describe summer conditions. These data will be used to help develop and improve algorithms to relate both optical (satellite) and acoustic (ADCP) backscatter to *in situ* TSM concentrations. Continuing ADCP measurements at A5 during the spring-summer (29 Mar.-9Aug.) of 2012 have significantly enhanced the A5 database.
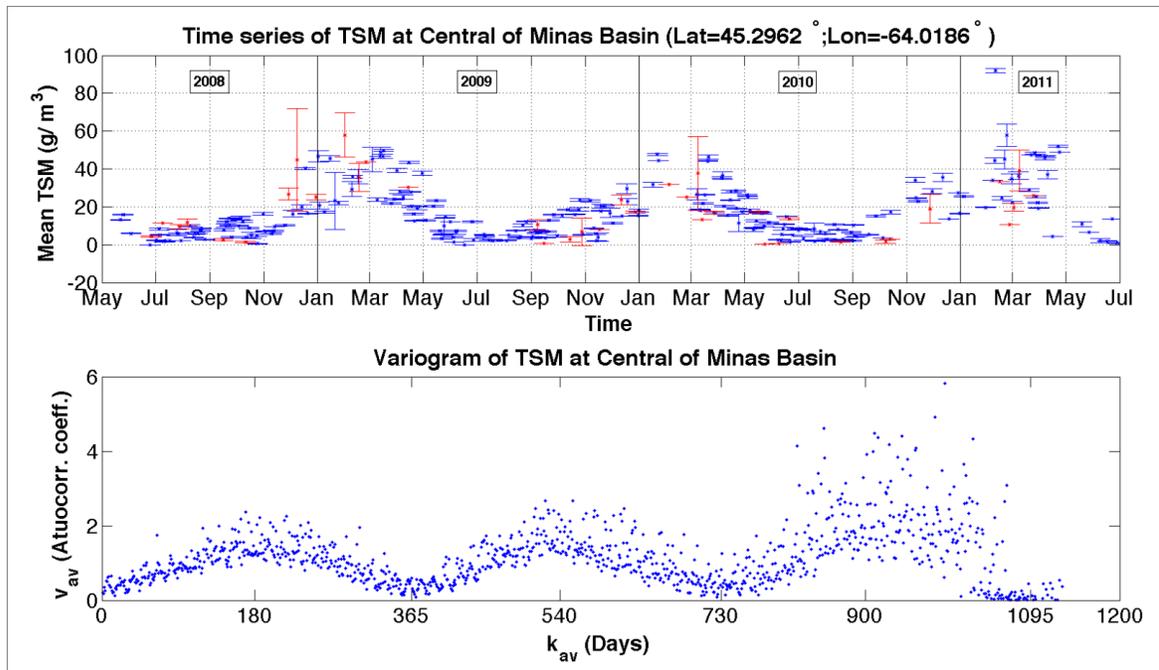
Figure 3. Time series of TSM derived from the MERIS satellite. The top panel shows 3 years of mean TSM in a 1-km box, which comprises 9 pixels in a MERIS image. The bottom panel shows a variogram of the time series. Smaller values indicate stronger autocorrelation. The variogram shows that concentrations are least correlated at time lag of approximately 6 months.

Ocean colour imagery of the upper Bay from the MERIS satellite has been analyzed by Jing Tao at Dalhousie University. Jing was provided with a set of relatively cloud-free images of Minas Basin by Cathy Porter and Carla Caverhill at Bedford Institute of Oceanography. Jing has produced time series of total suspended matter (TSM) in 1-km-square boxes throughout the Basin (Figure 3). With these time series, Jing has carried out temporal autocorrelation analysis. The analysis shows strong semi-annual variability in some parts of the Basin (Figure 3). Larger TSM is observed in mid-winter, and smaller TSM characterises mid-summer. The strength of this signal varies throughout the Basin, with the largest variation occurring in the centre of Minas Basin, and the smallest variation occurring in Cobequid Bay (Figure 4). Reproducing the magnitude and spatial patterns of semi-annual variability provides a good test for the numerical models. Jing also has estimated mean TSM of summer and winter seasons (Figure 5), which is used to evaluate model predictions. Jing has spent time (2 weeks in January, 2012) as a visiting student at Queen's University where she worked with Ryan Mulligan to compare the results of "winter" and "summer" model runs with Delft3D. The two model runs use three variables: critical erosion shear stress (τ_{cr}), settling velocity (w_s), and the erosion parameter (M) for muds to produce different TSM patterns in summer and in winter. The different values of $\tau_{cr,}$ w_s and M are used to model the effect of sedimentary biofilms on the erosional stability of sediments. Dr. Mulligan and Jing, working together, have evaluated the effect of those parameters on the model results and have determined that the seasonal signal seen in the satellite data can be reasonably reproduced. However, the model can't produce maps of where the seasonal signals are strong/weak. "Percent Difference" is a simple way to carry out a model-data comparison in

Minas Basin. The model underestimates mean TSM in the shallow areas in summer and overestimates them in winter, while data from the central basin shows reasonably good agreement (Figure 6).
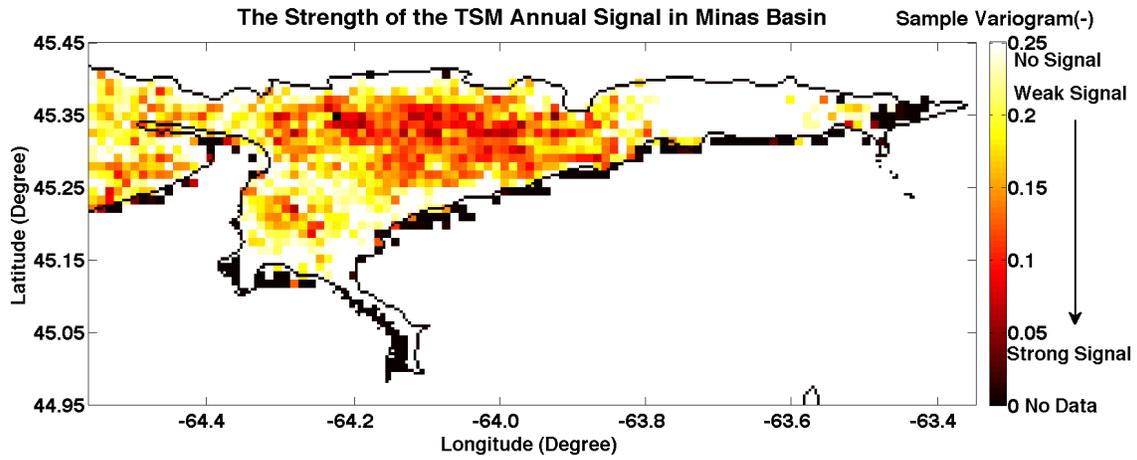
Figure 4. Spatial distribution of observed semi-annual change in TSM observed by the MERIS satellite. Lower values indicate larger semi-annual variation and are represented by darker colours.

a)
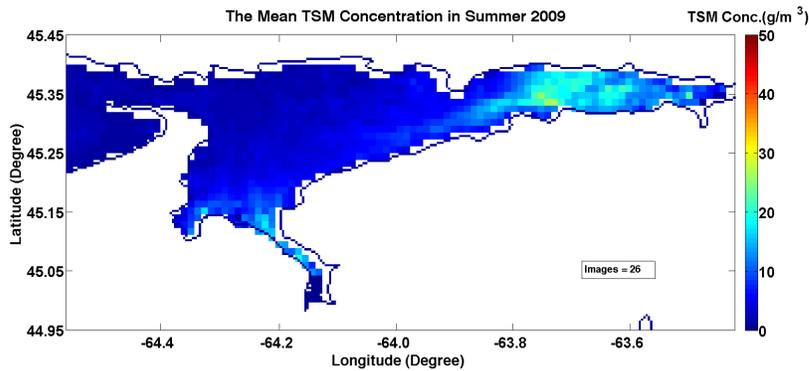
b)
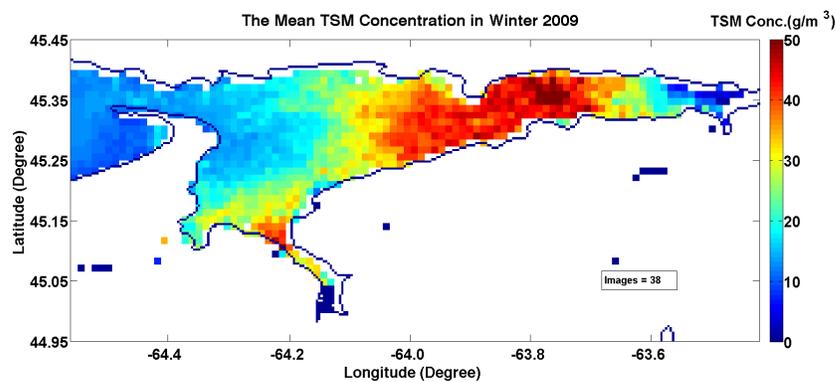
Figure 5. Mean TSM estimated from MERIS images during a two-month time series: a) summer, and b) winter, 2009. Largest concentrations, shown in warm colours, occur in Cobequid Bay. Smallest concentrations occur in Minas Passage.

a)

b)
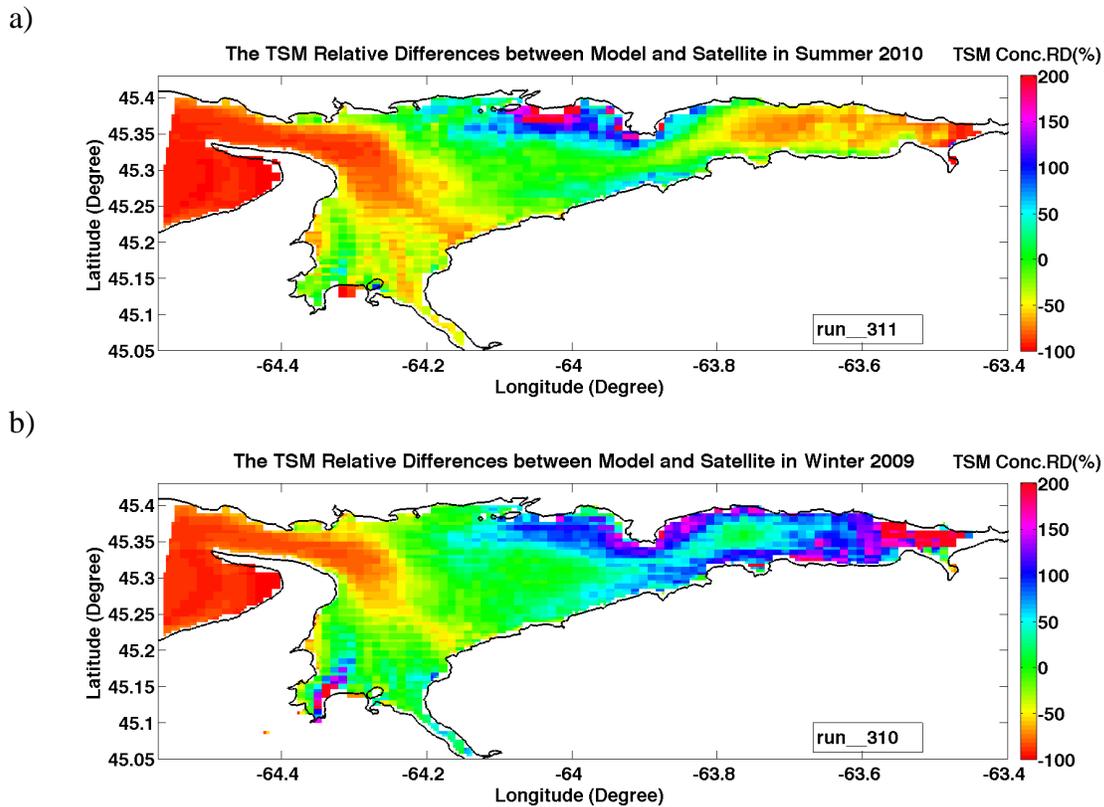
Figure 6. Quantitative comparisons between model and satellite data during a) summer, 2010 and b) winter, 2009. Positive values indicate the model overestimates the data, whereas negative values indicate the model underestimates the data.

In collaboration with Danika van Proosdij at Saint Mary's, sediment and current data collected on the Cornwallis River Estuary tidal flat have been investigated and used to evaluate model performance.

2.   Hydrodynamic model development
a) FVCOM

The FVCOM model has been successfully implemented on a new grid of the Upper Bay of Fundy. The new grid has ~200 m resolution in the critical Minas Passage area and incorporates the new high-resolution bathymetry. It should be noted that the new data display depth differences as much as 60 m from the existing nautical chart, i.e. parts of the channel are much deeper than the old chart depicts. Sediment grain size and textural data have been used to determine bottom roughness, a crucial input to the model. The inclusion of the new bathymetry and bottom roughness computations has enabled a better calibration than any model in this area to date.

The M_2 constituent constants at 10 water level stations in the upper Bay, obtained from FVCOM, are compared to observations in Table 1. As can be seen, the model tidal constants

agree well with the observations. For example, the difference of the amplitudes ranges from 0.24 to -0.04 m, the mean difference is 0.07 m, which is only 1.4% of the observed mean of 5.09 m. The range of the phase difference is -5.9º to 2.3º with a mean of -1.5º. The root-mean-squares (r.m.s) of the amplitude and phase difference are 0.11 m and 2.7º, respectively. The errors of the model figures, defined as the magnitude of the vector differences between model and observations on a polar plot of amplitude and phase [Dupont et al. (2005)], are also shown in Table 1. The amplitudes of model errors at 10 coastal stations vary from 0.09 to 0.45 m. The mean error is 0.22 m and the r.m.s is 0.25 m.

Tidal currents are usually difficult to reproduce in numerical ocean models. Present comparisons (Table 2) are very promising. The comparisons with data indicate very small errors in direction, magnitude, phase and ellipticity (minor axis).

Using the same station data, this model is also compared to two previous model studies. The first study (Dupont et al., 2005) used a 2-D high resolution finite element model with the aim of simulating the intertidal land-water interface in the upper Bay of Fundy. The second is the recent study of Karsten *et al.* (2008), in which a 2-D model version of FVCOM is used. To make sure the same stations are used in the comparison, the errors in their papers are recalculated according to the results listed in their papers. The r.m.s. error of Dupont's model is 0.28 m and the error of Karsten's model is 0.38 m, both larger than ours of 0.25 m. In our model the phase difference ranges from -5.9º to 2.3º, among which the modelled phase leads the observations at 3 stations and lags at 7 stations. It is interesting to note that the modelled tide in Karsten et al. (2008) leads the observations at all the 10 stations. In Dupont et al. (2005), however, the modelled tide lags the observations at all 10 stations.   The improvement in other constituents is also noticeable and may be attributed, at least in part, to the new sediment and bottom roughness data used in the model.

The modelled depth-averaged residual circulation is compared to its observed counterpart in Figure 7. Red arrows represent the recent data with good vertical resolution, whereas the green arrows are derived from earlier data representing only one or two vertical levels. Basically, the model results agree with the observations. For example, the directions of the eddies shown in the observations are successfully reproduced by model. Both the model and observations show the strong velocity shear along the northern and southern coast of Minas Passage. However, the magnitudes of the currents are found to be slightly overestimated or underestimated by model. A paper describing model comparisons with data of both hydrodynamic and sediment features has been published (Wu, *et al*., 2011).

The Western Minas mesh (Fig.8), that will be used to look in detail at sediment dynamics in the Cornwallis River area (Fig.8b), has been updated to better resolve the areas where Milligan and van Proosdij are concentrating their observations. It has been test run with M2 in a simple 2D drying model T-UGOm (Toulouse Unstructured Grid Ocean Model) and with multi-constituent tides using FVCOM. The latter tests have been made with configurations to run efficiently in parallel on multi-core computers.
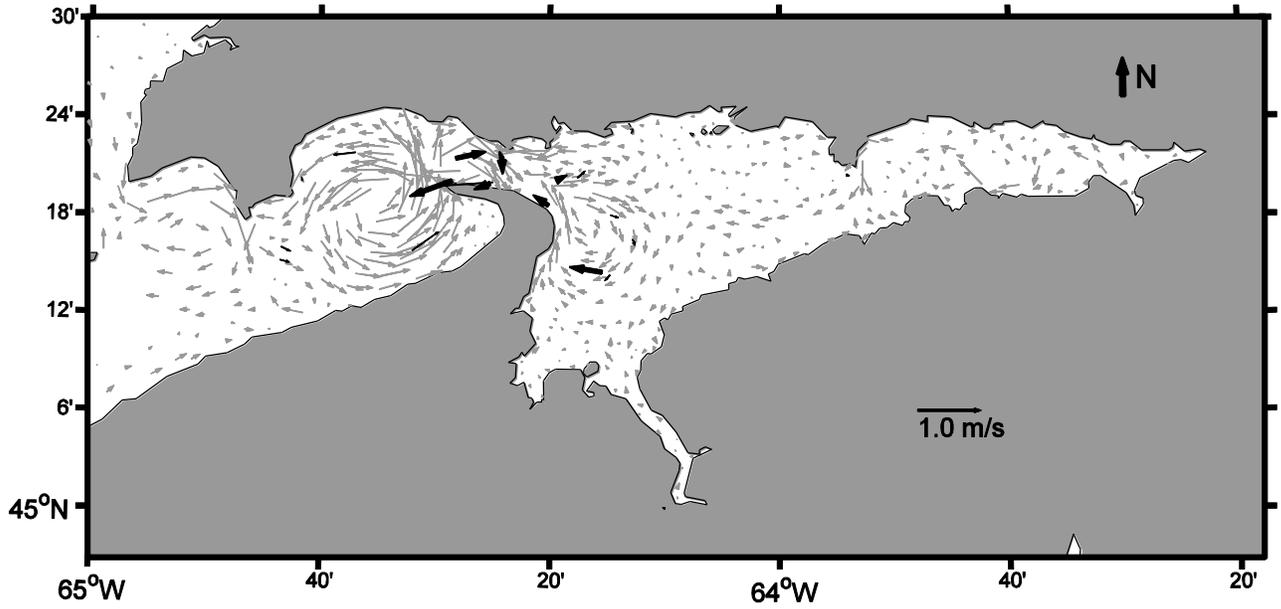
Figure 7. Depth-averaged residual flow. The thick black vectors are derived from recent current profile observations with high vertical resolution, the thin black vectors are based on early data with only one or two vertical levels and the gray vectors are the model results.
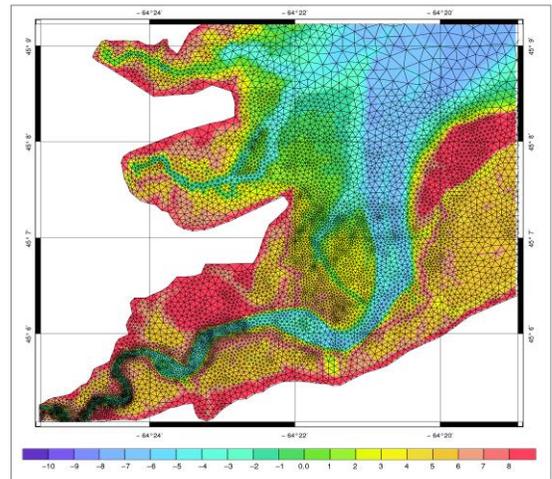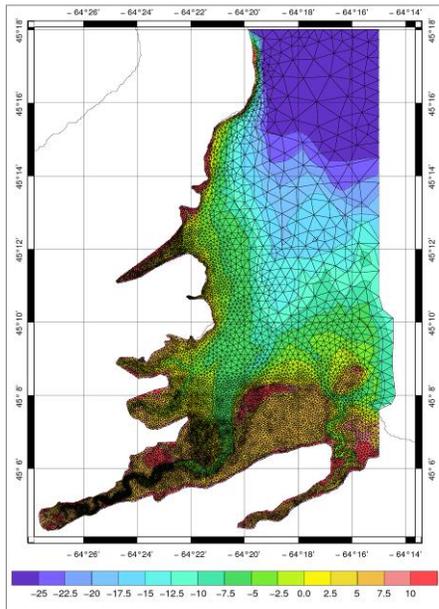
Figure 8 Fine-mesh FVCOM model grids for western Minas Basin (left) and Cornwallis River region (right).

Table 1. Observed and modelled amplitude and phase, and discrepancies of tidal levels for M2

Stations	Observed		Modelled		Difference		Errors
	Ampl. (m)	Phase (°)	Ampl. (m)	Phase (°)	Ampl. (m)	Phase (°)	
Isle Haute	4.15	99.2	4.00	103.4	0.15	-4.2	0.34
Chignecto	4.26	104.2	4.10	105.1	0.16	-0.9	0.17
Grindstone	4.86	104.4	4.62	107.4	0.24	-3.0	0.35
CumberlandBasin	4.74	104.6	4.64	106.7	0.10	-2.1	0.19
Cape d'Or	4.34	102.0	4.32	107.9	0.02	-5.9	0.45
Cobequid Bay	6.12	129.3	6.12	131.6	0.00	-2.3	0.24
Economy	5.92	125.4	5.96	124.8	-0.04	0.6	0.08
Minas Basin	5.54	120.8	5.53	118.5	0.01	2.3	0.23
Blomidon	5.36	116.7	5.25	115.8	0.11	0.9	0.13
Cape Sharp(new)	5.17	117.0	5.15	118.0	0.02	-1.0	0.09
Mean	5.04	-	4.97	-	0.07	-1.6	0.22
r.m.s	5.09		5.02		0.11	2.73	0.25

Table 2. Observed and modelled amplitude and phase, and discrepancies of tidal currents for M2

Stations	Observed				Modelled				Difference			
	Major Axis (m)	Minor Axis (m)	Inclination (°)	Phase (°)	Major Axis (m)	Minor Axis (m)	Inclination (°)	Phase (°)	Major Axis (m)	Minor Axis (m)	Inclination (°)	Phase (°)
1708	2.87	-0.10	162.0	209.3	2.97	-0.05	162.0	207.2	-0.10	-0.05	0.0	2.1
1709	1.93	-0.09	166.6	200.0	1.73	-0.07	165.4	196.3	0.20	-0.02	1.2	3.7
1710	2.13	0.08	167.7	219.4	2.41	0.07	168.9	227.6	-0.28	0.01	-1.2	-8.2
1711	2.19	-0.03	144.5	199.1	2.25	0.00	145.5	190.2	-0.06	-0.03	-1.0	8.9
1715	0.93	-0.22	116.1	203.6	0.97	-0.34	120.1	199.2	-0.04	0.12	-4.4	4.4
1735	0.87	-0.21	114.1	206.8	0.92	-0.25	115.0	207.8	-0.05	0.04	-0.9	-1.0
Site1	3.23	-0.06	163.2	217.3	3.16	-0.01	165.6	218.8	0.07	-0.05	-2.4	-1.5
Site3	2.61	-0.02	154.9	212.1	2.62	-0.01	159.4	209.8	-0.01	-0.01	-4.5	2.3
Site4	2.68	-0.02	158.7	210.2	2.65	-0.01	159.1	209.9	0.03	-0.01	-0.4	0.3
Mean	2.16	-0.07	149.8	208.6	2.19	-0.07	151.1	207.4	-0.03	0.0	-1.51	1.22
r.m.s.	2.29	0.12			2.32	0.15			0.13	0.05	2.36	4.62

b) Delft3D (hydrodynamics)

A second 3-dimensional numerical flow model (Delft3D) is being developed for simulating the hydrodynamics in Minas Basin. Delft3D (Lesser *et al*, 2004) uses a finite difference scheme that numerically solves the fluid momentum equations. A boundary-fitted grid in spherical coordinates has been developed for Minas Basin covering a domain of approximately 110 km in the east-west direction and 45 km in the north-south direction, with an open boundary across Minas Passage (18 km west of Cape Split). The grid has a horizontal resolution of 200 m, and the vertical resolution is variable with 10-layers in topography-following coordinates, a computationally efficient resolution.

Results include the set-up and testing of the hydrodynamic model, and comparisons of results with the FVCOM model results and with ADCP observations. As an example, Figure 9 shows the observed currents (speed and velocity components) and model predictions at ADCP site A5 over a period of four days in July, 2009. Model results at this site and other sites agree well with the observed tidal amplitudes and phases.

Delft3D results also compared well with the FVCOM model results. Both models predict a non-uniform distribution of currents across Minas Passage during the ebb tide and strong horizontal current shear with re-circulation during the flood stage of the tidal cycle.
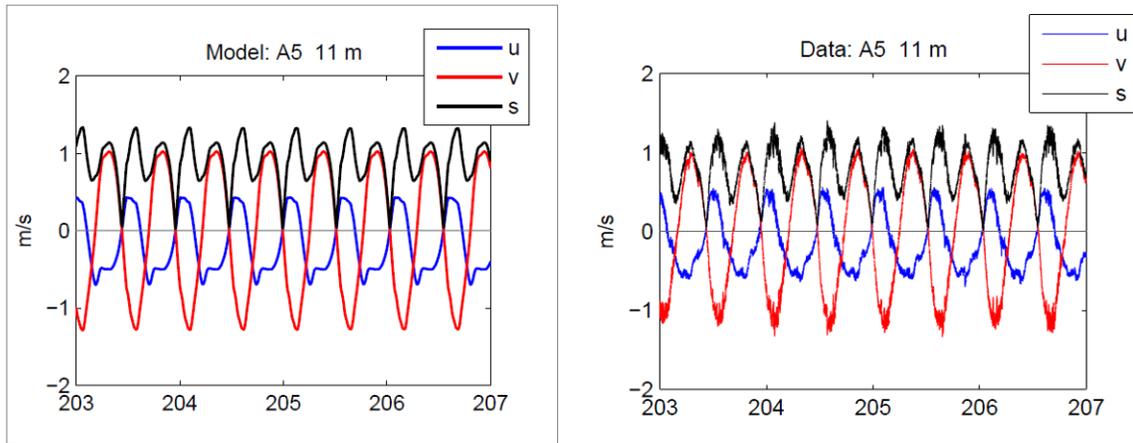
Figure 9: Comparison of observed horizontal current velocity components (u,v) and speed (s) time series at the 11 m depth at site A5 in the Southern Bight of Minas Basin. The x-axis indicates the Julian date in 2009 (July 22-26).

3.   *Sediment dynamics model development*

a) FVCOM

The sediment transport includes two components, bed load and suspended load. The bed load is calculated using the modelled bottom shear stress and the observed grain size data, and the results roughly agree with the observed features of the historical erosion and deposition observations in Minas Basin and Cobequid Bay. The transport of the suspended load is estimated using the modelled velocity field and the remotely-sensed surface sediment concentrations. As an example, the horizontal of suspended load transport is plotted in Figure 10a. During the flood and ebb periods, the transport direction of the suspended particulate load mainly follows the tidal currents. During flood tides, the suspension advances eastward with the currents, whereas during the ebb period, it retreats westward. The horizontal distribution of the transport during flood and ebb is relative uniform. The typical magnitude is about 0.5 kg m^{-1} s^{-1} and reaches 1.0~2.0 kg m^{-1} s^{-1} in western Minas Passage. However, the magnitude of the net transport of the suspension over an entire tidal cycle shows a strong spatial variation, despite the fact that it is clearly smaller than those in the flood or ebb periods separately. In Minas Channel, Minas Passage and Scots Bay, the magnitude of the transport is around 0.1 kg m^{-1} s^{-1} and only 0.01 kg m^{-1} s^{-1} in central Minas Basin and the Southern Bight. Model results are qualitatively compared to field observations. As we can see, the modelled results show a reasonable agreement with the observations. For instance, the sediment moves along the anticlockwise direction in Minas Channel and transports

westward in the western edge of Minas Basin. In Cobequid Bay, both the model and data show the sediment transport eastern direction.

The total transport of bed load plus suspended load is concentrated in Minas Channel and Minas Passage, where the magnitude of the transport flux is about 0.1~0.2 kg m^{-1} s^{-1} (Figure 10b). In the remaining areas, the magnitude is relatively small around 0.01 m^{-1} s^{-1}. In Minas Channel, the sediment movement shows an anticlockwise structure. The sediment in Minas Passage moves eastward into Minas Basin. The sediment in the eastern Minas Basin mainly moves to the central basin. In the Cobequid Bay, the sediment transports to the upper bay.

b) Delft3D (sediment dynamics)

Hydrodynamics model results suggests that fine sediments would remain in suspension throughout much of the Bay, since the initiation of motion of fine cohesive sediment (0.1-1.0 N/m^2) is typically exceeded. Critical areas in terms of sensitivity to changes in forcing conditions imposed by tidal structures include the tidal flats in the southern bight of Minas Basin and at the eastern end of Cobequid Bay. As mentioned above, the work of Jing Tao focuses on the comparison of satellite data with model results, and use autocorrelation analysis to determine and quantify the seasonal variability of surface suspended sediment.

The testing of sediment routines in Delft3D includes varying sediment properties and types (cohesive/non-cohesive) for different time periods. Figure 11 shows sample results for changes in surface suspended sediment concentrations due to water level variations over a tidal cycle. The results indicate strong variability over the cycle and transport of a sediment plume through Minas Passage (this example was initialized with a layer of cohesive sediment on the bed with a settling velocity of 25 mm/sec and a critical bed shear stress of 1000 N/m^2; no transport from rivers was included).

We have testedthe sediment transport formulations in Delft3D for suspension of bottom sediments by tidal currents for a variety of initial conditions, sediment types (cohesive and non-cohesive) and sediment properties (e.g. grain size, settling velocity, critical shear stress). Effort has been concentrated on getting the initial sediment conditions generally correct in Minas Basin and comparing with satellite imagery.
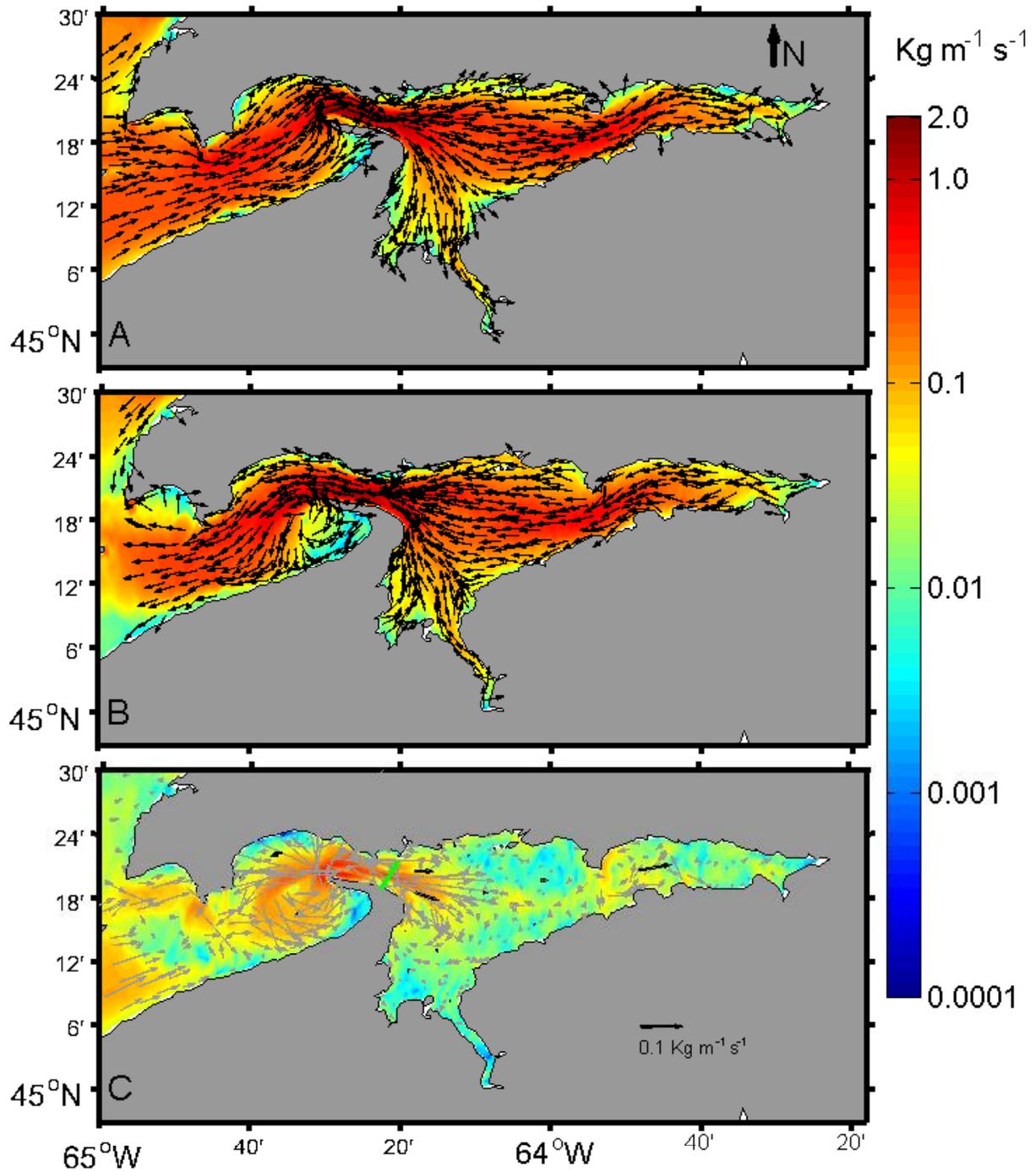
Figure 10a. Contour map of the suspended load transport rate flux (per unit cross-sectional distance) averaged during flood (A), ebb (B) and over the entire cycle (C). The black thick vectors in C represent the observed fluxes. The green vectors in C are the observed net suspended sediment transport (Amos and Joice, 197). The arrows in A and B indicate only the direction of the transport, but those in C indicate both magnitude and direction.
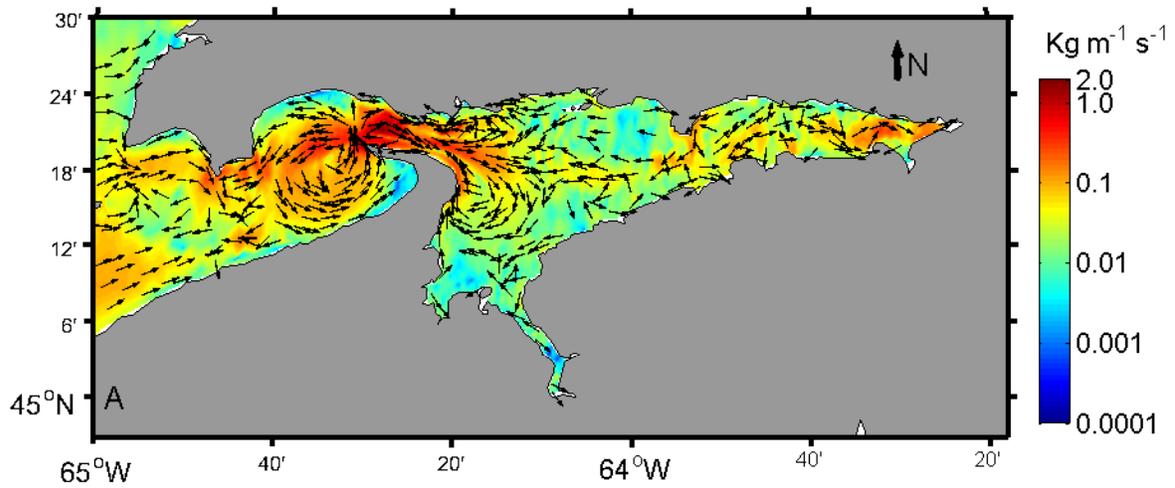
Figure 10 b. Total sediment transport flux. The arrows indicate the direction of the transport and colour contours indicate the transport rate.
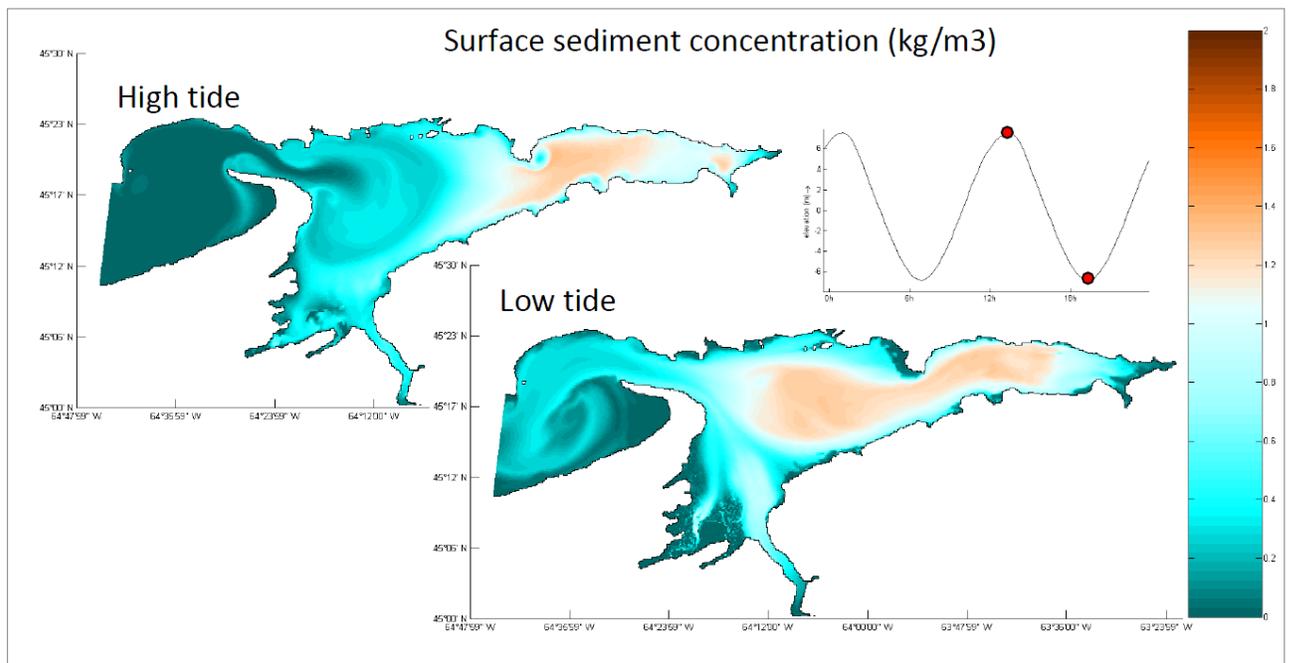
Figure 11 Initial test of Delft3D prediction of surface sediment concentrations for cohesive sediments.

An example of known bottom sediment textures from observations (reported in Greenberg and Amos, 1983) are shown in Figure 12a. Based on this, it can be noted that the several sediment types exist on the seabed and the pattern is complex. However, most sediments are non-cohesive (sands to gravels) with particles that have relatively high settling velocities.

Fine cohesive sediments (muds) occur in several locations around the rim of the basin, namely the Cornwallis River estuary, the Avon River channel, near Economy Point and in Scot's Bay. Based on this, a simple bi-modal distribution map has been developed for input to the model (Figure 12b). This consists of initial seabed of mud in water depths of 10 m and less (mean sea level) and sand in depths greater than 10 m. The resemblance of Fig 12a to 12b is striking, except that the model input has more fine sediment along the edges of the basin and in Cobequid Bay.

For the sand layer, a mean grain diameter (d_{50}) of 2 mm was used with the non-cohesive sediment formulation (Van Rijn, 2007a,b). Model results indicate that these particles become transported as bedload and suspended load during ebb and flood phases of the tide, with highest concentrations in Minas Channel where currents are strongest. However the coarse particles have a high settling velocity and sink out of suspension with slackening of the tidal currents.

For the cohesive intertidal mud layer, a settling velocity of 0.1 mm/s was used, corresponding to a grain size of less than 100 μm, and the critical shear stress for erosion (τ_{cr}) was varied based on values determined by Amos (1992) for bed sediment samples on the tidal flat of the Cornwallis river estuary. Across the 2.5 km wide mudflat they measured *in situ* bed shear stresses of up to 0.1-7.5 N/m^2 (in July and August, 1989-1990), which notably is 1-2 orders of magnitude larger than for other studies [e.g. Greenberg and Amos (1983) use 0.1-0.2 N/m^2] and for other estuaries.

An example of the model simulated surface suspended sediment concentrations at different tidal phase in a single tidal cycle are shown in Figure 13, forced by M2 tides at the open boundary and using a high critical bed shear stress $\tau_{cr} = 5$ N/m^2. In comparison with satellite observations at similar stages of the tide (Figure 14), the model adequately simulates some important sediment transport phenomena, including:

- Higher surface TSM in the source areas, which include the tidal flats and river mouths in Cobequid Bay and the Southern Bight of Minas Basin.

- Lower TSM in the central part of Minas Basin and Minas Passage and Minas Channel

- Larger areas and higher concentrations of suspended materials at low tide and on flood tide.

At A5, the site of the ADCP deployment, the model predicts the variability in TSM to be 0.1-0.5 g/m^3 over the tidal cycle (note that this suspended sediment is from shallow intertidal areas and has advected to the A5 site). This may well represent summer sediment conditions, with high cohesion due to biological trapping of the sediments. In comparison, the satellite observations of surface TSM at A5 were also low (1-5 g/m^3) in October 2008.

Decreasing the τ_{cr} to a lower value (1 N/m^2) to represent winter sediment conditions (lower cohesion due to no biological re-working) results in an increase in surface TSM variation to 1-50 g/m^3 at A5 over the tidal cycle with the same tidal forcing. Values observed by satellite were also higher (10-30 g/m^3) in winter 2009.

The results of three model runs for varying τ_{cr} are summarized in Figure 15, with higher suspended sediment concentrations and variability at A5 for lower critical bed shear stress. Therefore the system is very sensitive to τ_{cr}, and a seasonal change in sediment properties

that increases the cohesion causes an order-of-magnitude change in sediment volume in suspension.
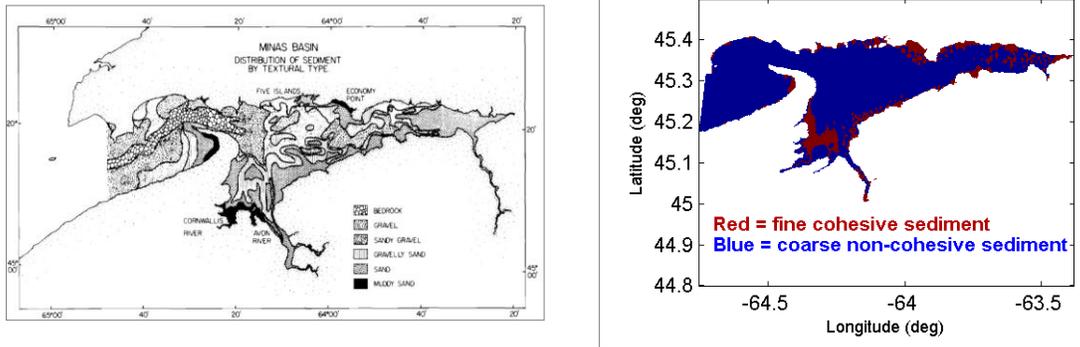
Figure12. Bottom sediment texture maps, a) from observations and reported in Greenberg and Amos, 1983; b) simple bi-modal distribution for present model input.
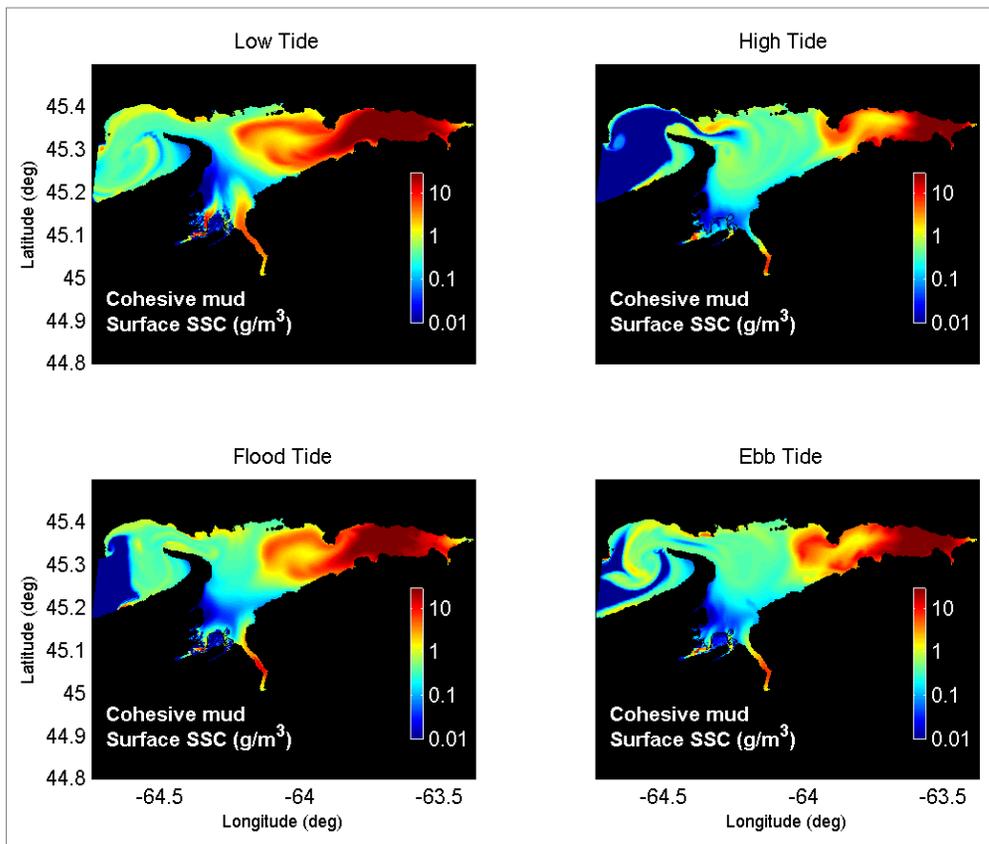
Figure 13: Model simulated surface suspended sediment concentrations at different tidal phase in a single tidal cycle, initiated with cohesive sediments in shallow areas (MSL 10 m and shallower) and forced by M2 tides at the open boundary.
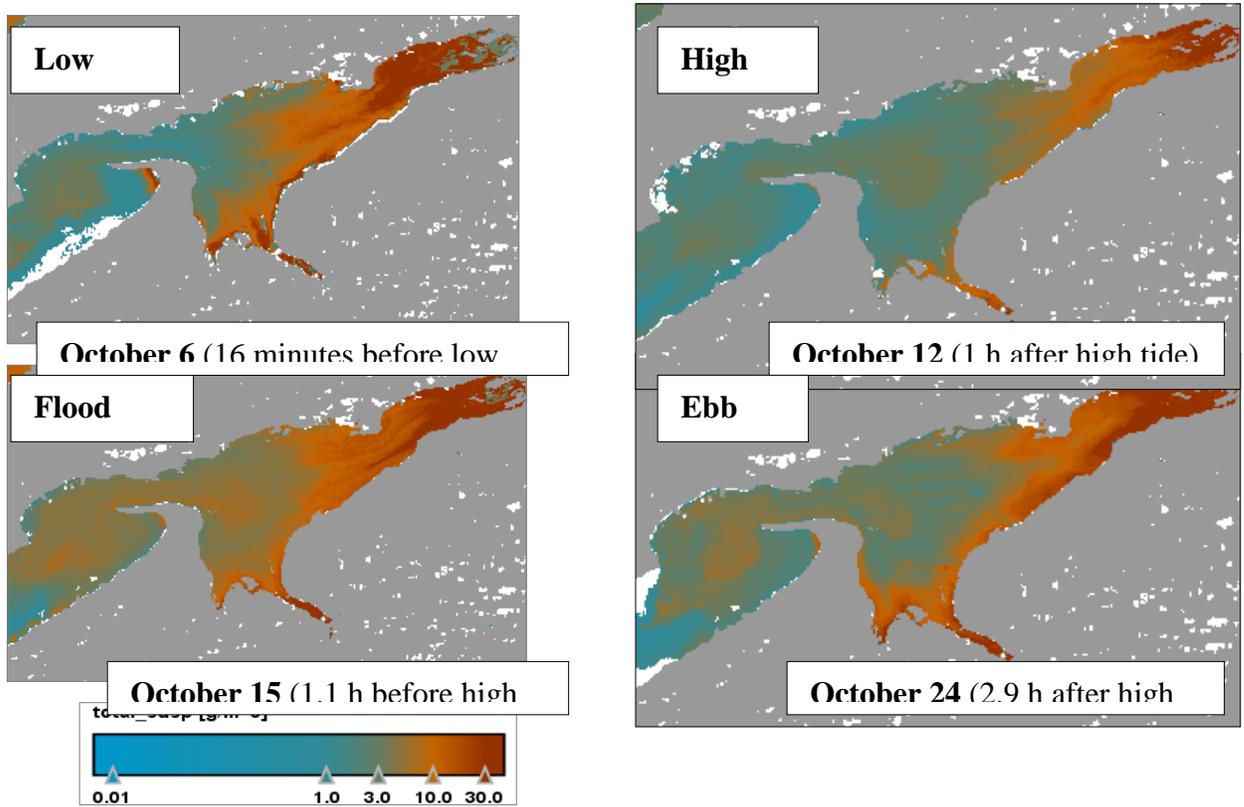
Figure 14: Surface suspended sediment concentrations (SSC) from MODIS imagery at various stages in the tidal cycle through October 2008 (from G. Budgen, BIO).
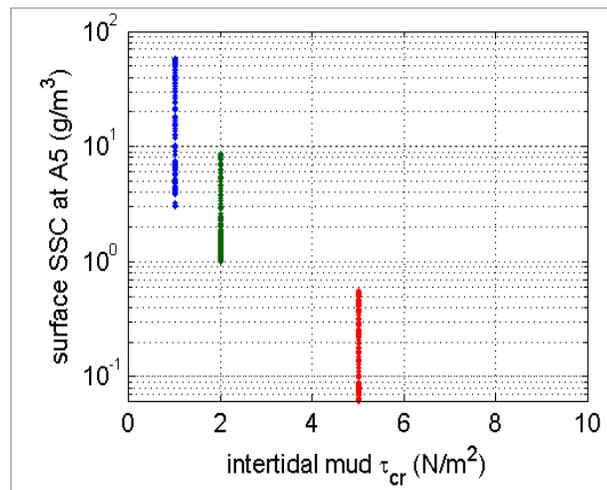
Figure 15: Model prediction of the surface SSC variability at A5 over a tidal cycle for different critical shear stress values of cohesive muds in the intertidal zones.

c) Delft3D (wave-driven sediment resuspension on the tidal flats)

Minas Basin is a semi-enclosed estuary that is regularly exposed to wind forcing, in addition to strong tidal forcing. Storm events may have strong effects on sediment transport, with winds that generate fetch-limited surface waves. These waves may be important for resuspension over the shallow tidal flats in the basin, by inducing wave orbital velocities at the seabed that in addition to tidal currents, create strong shear stresses on the bed. Surface waves are known to be important in the resuspension of bottom sediments and changes in suspended material concentrations in the overlying water column, and transport in tidal estuaries (Ward, 1984). Previous modelling studies in Minas Basin have not considered the effect of surface waves on sediment dynamics. We developed a surface wave model for Minas Basin and coupling it to the existing Delft3D (Lesser, 2004) hydrodynamic and sediment model. This has been accomplished using the SWAN (Booij, 1999) shallow-water spectral wave model, and the coupled models are used to identify the roles of the surface waves that cause resuspension and the tidal circulation responsible for transport of suspended materials.

Results from three scenarios are presented here, including model runs using: i) M2 tidal forcing only; ii) M2 tidal forcing plus winter wind conditions (assuming no ice cover); iii) M2 tidal forcing plus summer wind conditions. Winter and summer wind conditions are idealized cases, developed from climatological summaries (Eid *et al*, 1991). The wind and wave climate statistics were derived from ship-of-opportunity wind data, real-time buoy and rig data sets covering a time period from 1957-1988. The "winter case" was estimated from the 50% wind speed exceedence value for the month of January (12.9 m/s from 315°N in the Bay of Fundy, blowing across Minas Basin from the NW). The "summer case" was estimated from the 50% wind speed exceedence value for the month of July (7.7 m/s from 225°N in the Bay of Fundy, blowing along Minas Basin from the SW). With a significant seasonal change in mean wind speed and direction, the winter conditions could promote significantly higher wave heights and resuspension rates along the southern shore of Minas Basin. To test this, wind forcing was applied (after a spin-up period with no winds) as a daily constant step function for a duration of 4 days, representing an average storm that persists over several tidal cycles. Sediment properties for these cases were held constant with a spatially varying bimodal distribution that included non-cohesive sand ($d_{50} = 2$ mm) and cohesive mud ($\tau_{cr} = 1$ N/m^2, $w_s = 0.1$ mm/s, $d_{50} = 100$ μm).

The results at the observation site A5 are shown in Figure 16. The larger waves in the winter case ($H_s = 1.1$ m, $T_p = 4.4$ s) induce nearly twice the TSM at A5 compared to tide only case (e.g. 85 g/m^3 with waves; 45 g/m^3 without waves). The summer wave conditions ($H_s = 0.5$ m, $T_p = 3.2$ s) result in a reduction in TSM at A5 compared to the no wind run. In this case the wind induces a small component of transport to the east, and slightly reduces the sediment concentration in the southern bight. Predicted sediment concentrations on the tidal flats (e.g. the mouth of the Cornwallis River) are an order of magnitude larger than at A5 (28 m depth). The relatively small and short-period waves have a significant effect on the resuspension of bottom sediments by increasing the bottom shear stress over the tidal flats. This is most pronounced at low tide. The spatial difference in TSM between tide-only and winter wave model results at low tide is shown in Figure 17, and indicates that resuspension is enhanced by waves along the south coast and in the southern bight of Minas Basin. The tidal currents are primarily responsible for transporting the sediments once suspended, but the

combination of tidal currents and wave orbital velocities influence the resuspension of bottom material. These results indicate the importance of wind and wave processes in the suspended sediment distribution in Minas Basin, and suggest that seasonal signals in TSM are influenced by seasonal changes in meteorological forcing.
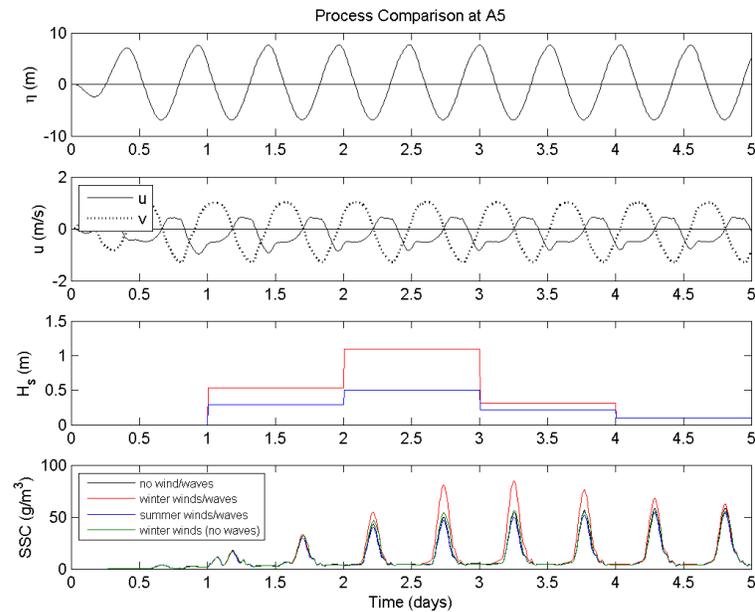
Figure 16: Model predictions of mean water surface elevation, current velocity, significant wave height and surface sediment concentrations at site A5 for the test cases: tides only; tides plus winter waves; tides plus summer waves; and tides plus wind-driven currents (no waves).
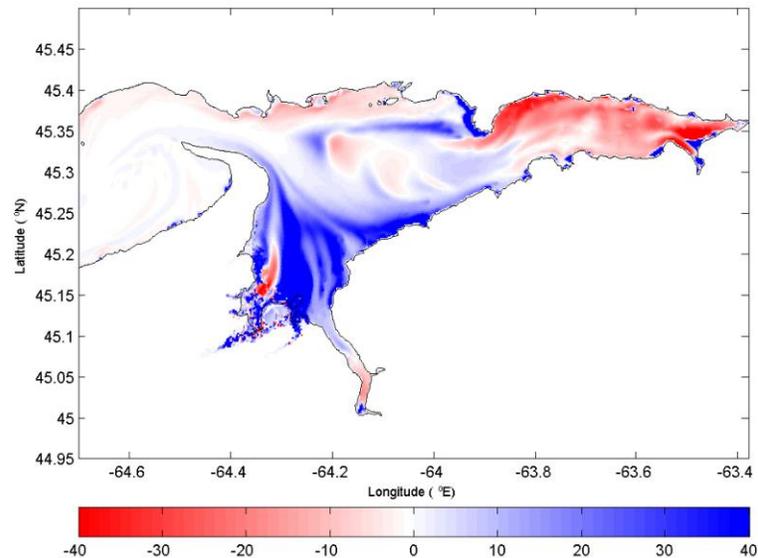
Figure 17: Difference between models runs in sediment concentration at the sea surface (g/m^3) at low tide. The case with tide only was subtracted from the case with tide plus winter waves, therefore BLUE represents increased in TSM due to waves and RED represents decreased TSM between the runs.

d) FVCOM assessment of environmental impacts of tidal power extraction

Environmental impacts of tidal power extraction in the upper Bay of Fundy have been investigated with a three-dimensional hydrodynamic model, in which the presence of in-stream turbines is simulated by an extra term, namely momentum drag, in the standard momentum equations (Wu *et al*, 2012). The method is found to be reasonably efficient in representing velocity changes due to the tidal energy extraction. The preferred site for tidal power extraction in Minas Passage is investigated first based on engineering constraints of tidal speed, water depth, tidal bi-directionality and bottom slope, and then a series of numerical tests is performed with various arrangements of turbines, from a single isolated turbine to a commercial-scale "turbine farm", with the aim of understanding changes in tidal regimes and sediment transport due to the presence of turbines. The model results indicate that the presence of turbines reduces the tidal speed not only in the downstream, but also in the upstream because of the alteration of the tidal flow by the turbines. The existence of turbines significantly impedes tidal flows at the turbine sites, both ahead of the turbines and in their wake flow areas, but most of the blocked water passes around the turbines and eventually enters Minas Basin through the deep channel along the southern shore of Minas Passage (see example for linear array, Figs 18,19). At the turbine sites, the magnitude of the depth-averaged tidal velocity decreases by 10~20% of the natural tidal flow. On the contrary, in the southern deep channel, tidal speed increases by a comparable magnitude (Figure 20). Compared to the changes in tidal currents, the magnitude of changes in tidal elevation is much smaller, only ~0.5 to 1% of the tidal amplitudes in the natural case (Figure 21). Sediment was found to move less actively at the turbine sites and in their wake flow areas due to the kinetic energy reduction. The decreased relative magnitudes of the transport rates reach 50%. However, the existence of the turbines increases the transport rates in nearshore areas along both the northern and southern coast of the Passage and the relative magnitudes reach 100%. Specifically, the consequence of these changes is that less coarse sediment moves into the central Minas Basin, but more coarse sediment is transported to Southern Bight through the deep channel along the southern side of Minas Passage. The sediment transport rate increases dramatically (>100%) in the coastal water of Greville Bay, and at the top of Scots Bay (Figure 22) but the absolute values of the sediment transport rate are relatively small.
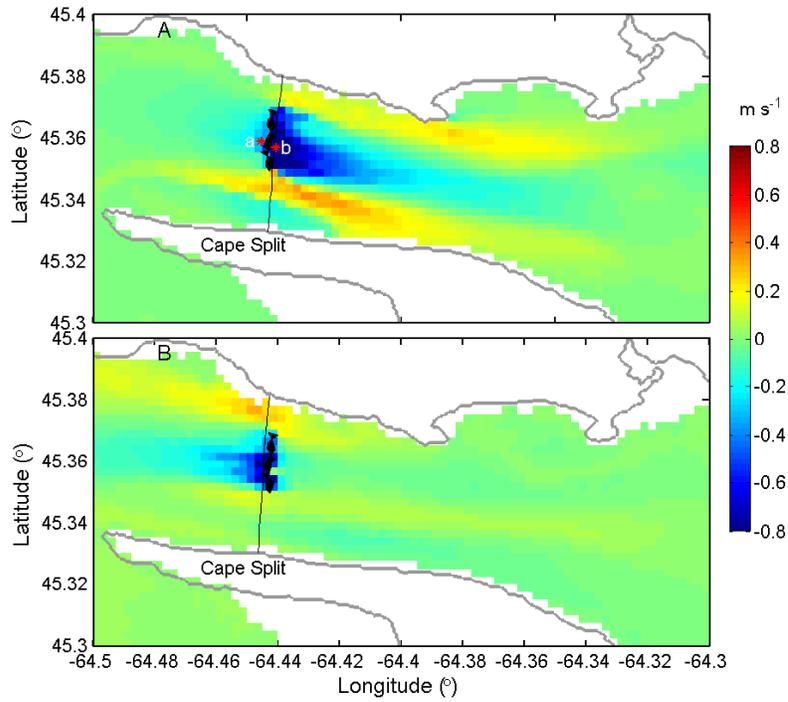
Figure 18. Example of tidal current speed change at 10m above seabed at mid-flood (A) and mid-ebb (B) due to a linear array of turbines in Minas Passage. Black triangles indicate turbine positions and black line shows position of vertical section in Fig. 19.
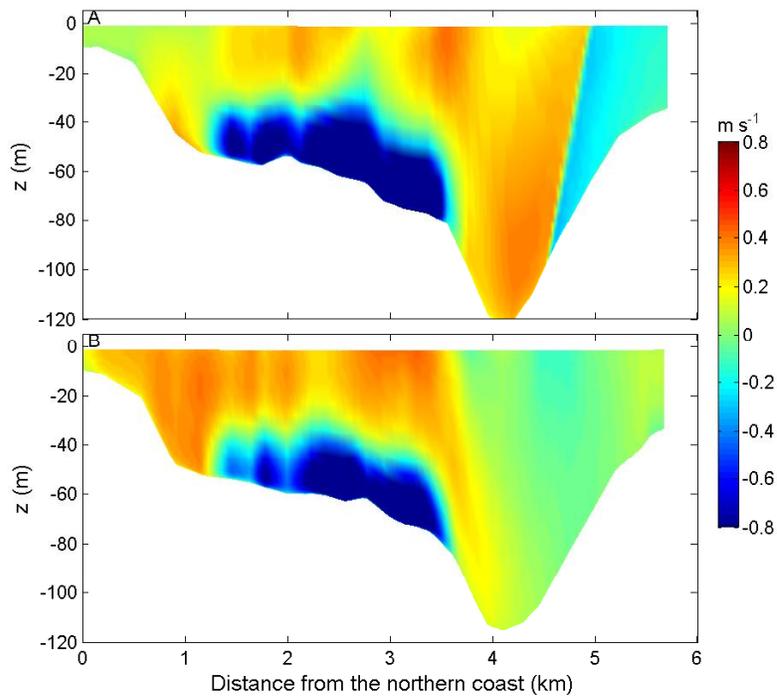
Figure 19. Vertical distributions of tidal current speed change along sections in Fig. 18.
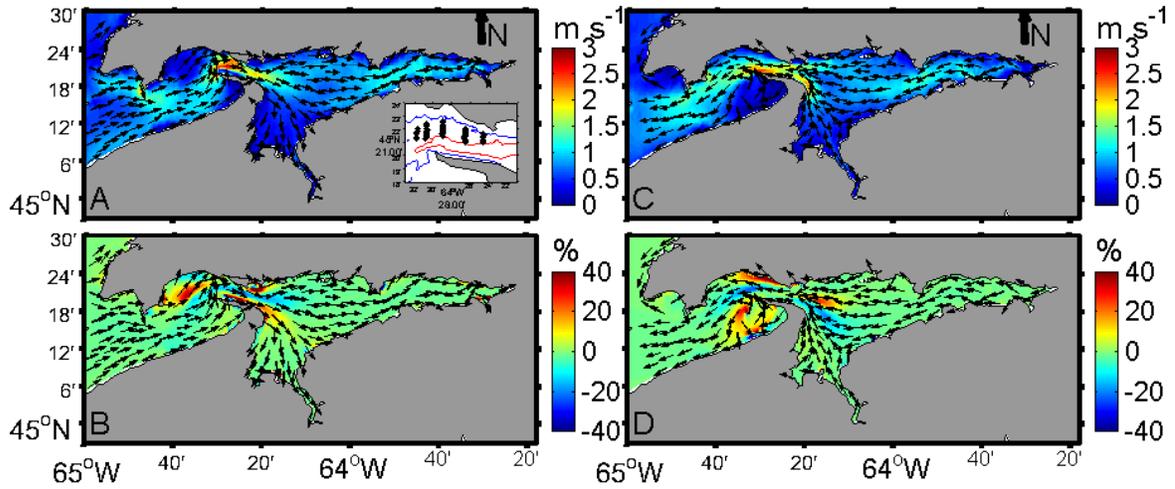
Figure 20. Mean depth-averaged velocity during flood (A), ebb (C) and their changes (defined defined as $(U_T-U_N)/U_N \times 100\%$, where U_T indicates the velocity in the case with turbine and U_N stands for the velocity without turbines) in (B) and (D), respectively. The figure at the right corner in (A) shows turbine sites. The blue and red contour lines indicate the 30 and 80 m bathymetric contours, respectively. The arrows in the figure only represent the directions of the tidal currents from model run with turbines, and their lengths are not scaled by the current magnitudes.
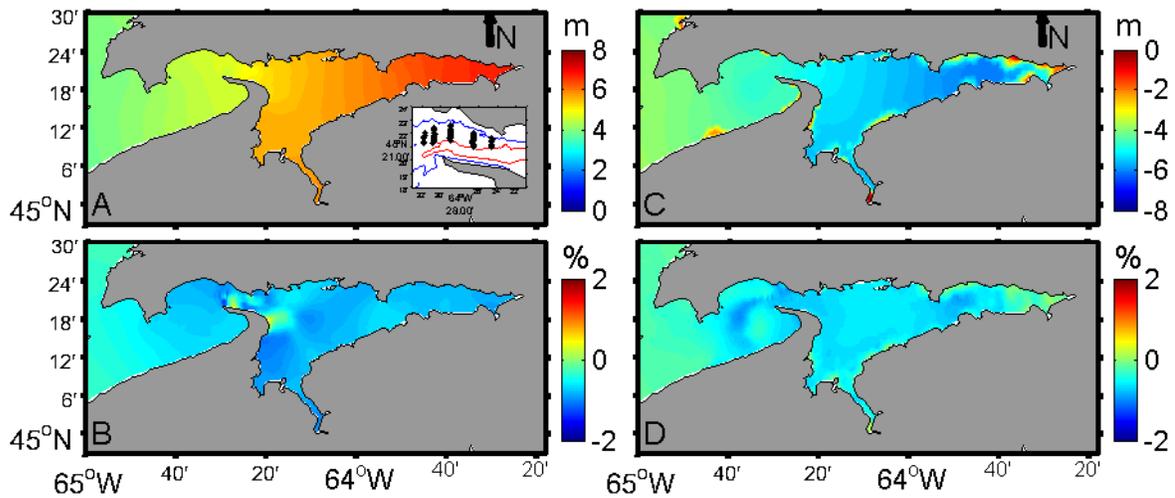
Figure 21. Mean high tide (A), mean low tide (C) and their proportional changes (defined in the text) in (B) and (D), respectively. The figure at the right corner in (A) shows turbine sites. The blue and red contour lines indicate the 30 and 80 m bathymetric contours, respectively.
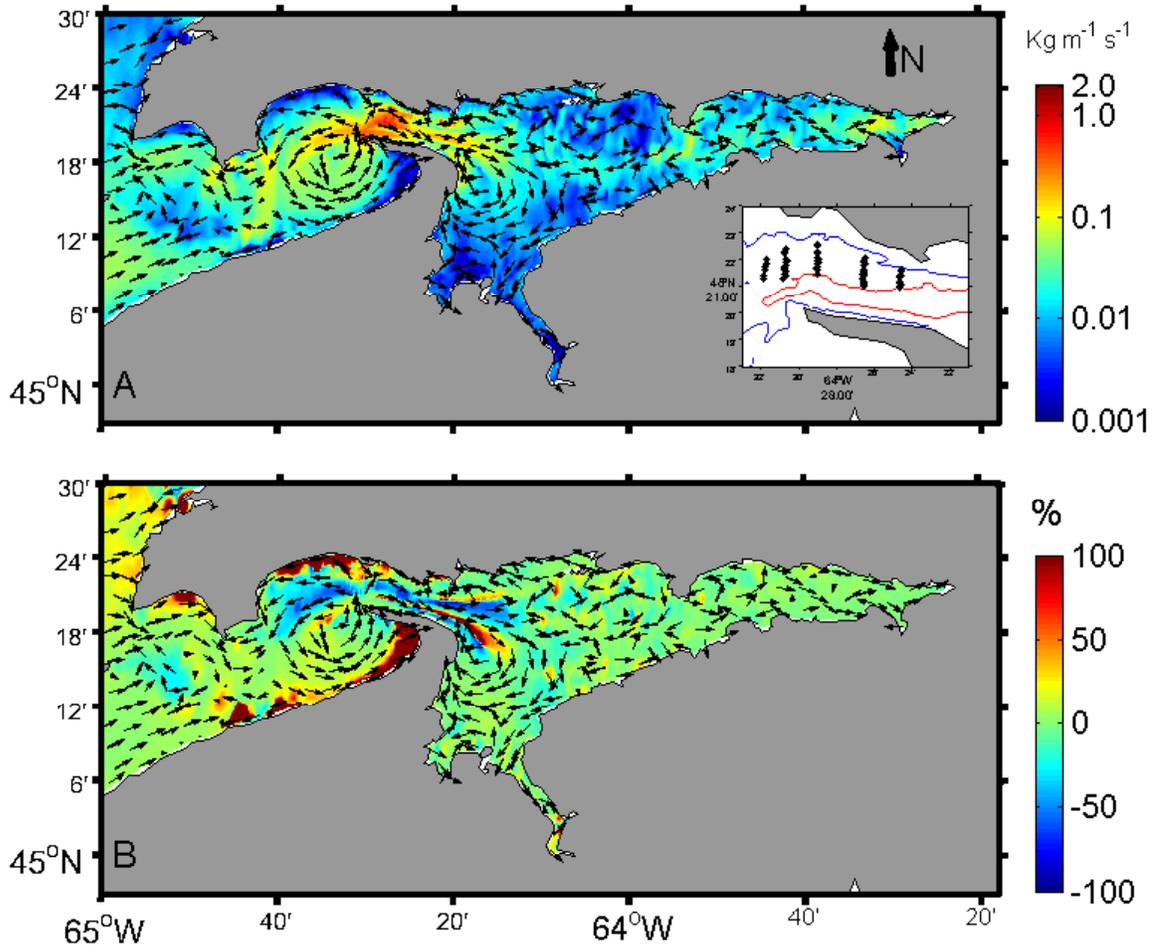
Figure 22. Mean total load transport rate in tidal cycles (A), and changes (B). The figure at the right corner in (A) shows turbine sites. The blue and red contour lines indicate the 30 and 80 m bathymetric contours, respectively. The arrows in the figure only represent the directions of the sediment transport rate from model run with turbines.

Dissemination and Technology Transfer

Technology Transfer: The results and processed data from the ADCP deployments in the upper Bay of Fundy have been freely shared with both industry (FORCE) and other project proponents (e.g. at Dalhousie U. and Acadia U.)

Events: Information from this project has been shared on several occasions including:

- ♦ FORCE, OEER/OETR Information Sharing Meeting, 29 January 2010 at the Bedford Institute of Oceanography, Dartmouth, NS
- ♦ NS Energy Research & Development Forum, 26-27 May 2010 at the World Trade and Convention Centre, Halifax, NS
- ♦ Results of this work have also been shared at meetings of FORCE, EMAC (Environmental Monitoring Advisory Committee), FERN (Fundy Energy Research

Network) and its predecessor committees, and DFO's renewable energy working group (TEER).

- ♦ Though scientific seminars, results of this work have been shared with scientists at leading institutions and governmental organizations across North Carolina and Ontario. These include East Carolina University, the University of North Carolina Institute of Marine Sciences, the U.S. National Oceanographic and Atmospheric Administration, the U.S. Army Corps of Engineers, Queen's University, the University of Ottawa, and the Royal Military College of Canada.
- ♦ OEER/FORCE Tidal Energy Workshop, Wolfville NS, October 13-14, 2010
- ♦ Tidal Research Interpretive Material – FORCE Visitor Centre, *Video interview with P.C. Smith*, April 2011
- ♦ *Conference presentation*: Mulligan, R.P, P.C. Smith, P.S. Hill, J. Tao, Y.Wu, G. Bugden and D. van Proosdij. Suspended sediment processes in Minas Basin, the Bay of Fundy. Presented in the session on Sediment Transport and Deposition in Lakes, Estuaries, and Shallow Shelves at Ocean Sciences 2012, Salt Lake City, UT, USA;
- ♦ *Conference presentation*: Wu Y., J. Chaffey, D. A. Greenberg and P.C.Smith, Tidally-induced sediment transport in the Upper Bay of Fundy: a numerical study. CMOS2011, Victoria, BC; Wu Y., J. Chaffey, D. A. Greenberg and P.C.Smith, Environmental impacts of tidal power extraction in the upper Bay of Fundy. CMOS, 2012, Montreal, QC.
- ♦ FVCOM model results used by geophysicists J. Shaw (NRCan) and M. Li (NRCan) to interpret tidal scour regime in Minas Passage (Shaw, *et al*, 2012; Li, *et al*, 2013)
- ♦ *Conference abstract accepted*: Mulligan, R.P, P.C. Smith, P.S. Hill, and D. van Proosdij. Effects of tidal power generation on hydrodynamics and sediment processes in the upper Bay of Fundy. Accepted in Speciality Conference on Coastal, Estuary and Offshore Engineering at Canadian Society for Civil Engineering 2013 Annual Conference, May, 2013, Montreal, QC.

Publications

Lee, K., P.C. Smith, R. Parrott. 2008. BIO contributes to the development and regulation of Canada's ocean renewable energy industry. *Bedford Institute of Oceanography in Review, 2008.* p.4-11.

Wu, Y., J. Chaffey, D.A. Greenberg, K. Colbo, and P.C. Smith. 2011. Tidally-induced sediment transport in the Upper Bay of Fundy: a numerical study, *Cont. Shelf Res,* doi:10.1016/j.csr.2011.10.009.

Wu, Y., J. Chaffey, D.A. Greenberg, and P.C. Smith. 2012. Environmental impacts of tidal power extraction in the upper Bay of Fundy, *Estuaries and Coasts*, submitted.

Shaw J., B. J. Todd, M.Z. Li, and Y. Wu. 2012. Anatomy of the tidal scour system at Minas Passage, Bay of Fundy, Canada. Marine Geology, 323-325, 123-134.

Li, M.Z., J. Shaw, B.J. Todd, V.E. Kostylev, and Y. Wu. 2013. Geomorphology and sedimentary processes of large bedforms near Cape Split, Upper Bay of Fundy, Canada. *In preparation*.

Mulligan, R.P, P.C. Smith, P.S. Hill and J.Tao. Hydrodynamics and suspended sediments in Minas Basin, the Bay of Fundy. *In preparation*, with plans to submit to *Estuarine, Coastal and Shelf Science* in 2013.

Tao, J. Seasonal variability of total suspended matter in Minas Basin, Bay of Fundy. M.Sc. thesis, Dalhousie University. *In preparation*, with plans to defend in 2013.

References

Amos, C.L. and G.H.E. Joice. 1977. The sediment budget of the Minas Basin, Bay of Fundy, N.S. Bedford Institute of Oceanography, Data Series Report, BI-D-77-3, 274pp.

Amos, C. L., Daborn, G.R., Christian, H.A., Atkinson, A., and Robertson, A., 1992. In situ erosion measurements on fine-grained sediments from the Bay of Fundy, Marine Geology, 108(2), 175-196.

Booij, N., Ris R.C., and Holthuijsen, L.H. (1999). A third-generation wave model for coastal regions, Part I, Model description and validation. *J. Geophys. Res.*, 104: 7649-7666.

Dupont, F., C.G. Hannah, and D. A. Greenberg. 2005. Modelling the sea level in the Upper Bay of Fundy. *Atmosphere-Ocean, 43(1)*, 33-47.

Eid, B., Dunlap, E., Henschel, M., and Trask, J., 1991. Wind and wave climate atlas, Volume 1: the east coast of Canada. *Transport Canada Publication* No.TP 10820E.

Greenberg, D. A., and Amos, C. L., 1983. Suspended Sediment Transport and Deposition Modeling in the Bay of Fundy, Nova Scotia - a Region of Potential Tidal Power Development, *Can. J. of Fisheries and Aquatic Sci.,* 40(suppl. 1) 20-34.

Karsten, R.H., J.M. McMillan, M.J. Lickley, R.D. Haynes. 2008. Assessment of tidal current energy in the Minas Passage, Bay of Fundy. *Pro. IMech E 222, Part A, J. Power and Energy*, 493-507.

Lesser, G., J. Roelvink, J. van Kester, and G. Stelling (2004), Development and validation of a three-dimensional morphological model, *Coastal Eng., 51*, 883– 915.

Long, B.F.N. (1979). The nature of bottom sediments in the Minas Basin system, Bay of Fundy. Bedford Institute of Oceanography Data Series, BI-D-79-4, vi, 101p..

Parrott, D.R., B.J. Todd, J. Shaw, J.E. Hughes Clarke, J. Griffin, B. MacGowan, M. Lamplugh, and T. Webster. 2008. Integration of multibeam bathymetry and LIDAR surveys of the Bay of Fundy, *Canada. Proc. Can. Hydrogr. Conf. and Nat. Surveyors Conf. 2008*, Paper 6-2, 15pp.

Van Rijn, L.C., 2007a. Unified view of sediment transport by currents and waves I: Initiation of motion, bed roughness, and bed-load transport, *J. of Hydraulic Eng.*, 133(6), 649-667.

Van Rijn, L.C., 2007b. Unified view of sediment transport by currents and waves II: Suspended transport, *J. of Hydraulic Eng*., 133(6), 668-689.

Ward, L.G., Kemp, W.M. and Boynton, W.R., 1984. The influence of waves and seagrass communities on suspended particulates in an estuarine embayment. *Mar. Geol*., 59: 85-103.